Advanced Composite Materials
Publication details, including instructions for authors and subscription information:
http://www.tandfonline.com/loi/tacm20

Smart manufacturing of low-cost integrated panel by resin-transfer molding

Takashi Ito , Kenjiro Yamagishi , Ikuo Okumura , Shintaro Kitade & Yasuhiro Shigegaki

Version of record first published: 02 Apr 2012.

To cite this article: Takashi Ito , Kenjiro Yamagishi , Ikuo Okumura , Shintaro Kitade & Yasuhiro Shigegaki (2004): Smart manufacturing of low-cost integrated panel by resin-transfer molding, Advanced Composite Materials, 13:1, 57-66

To link to this article: http://dx.doi.org/10.1163/1568551041408804

Adv. Composite Mater., Vol. 13, No. 1, pp. 57–66 (2004)

Smart manufacturing of low-cost integrated panel by resin-transfer molding

TAKASHI ITO *, KENJIRO YAMAGISHI, IKUO OKUMURA, SHINTARO KITADE and YASUHIRO SHIGEGAKI

Ishikawajima-Harima Heavy Industries Co., Ltd., 1, Shin-Nakahara-cho, Isogo-ku, Yokohama 2358501, Japan

Received 18 July 2003; accepted 22 March 2004

Abstract—We proposed a smart manufacturing system for resin transfer molding (RTM). Numerical simulation was used to predict the resin-flow behavior and determined the preliminary process conditions. The injection pressure was controlled with a dielectric sensor, which monitored the resin-flow front. This approach was experimentally demonstrated by fabricating an access door panel model of a fuselage structure.

Keywords: Smart manufacturing; resin transfer molding; FBG sensor; numerical simulation; dielectric sensor.

1. INTRODUCTION

Resin-transfer molding (RTM) is applied to many kinds of fiber-reinforced plastic (FRP) products in the civil, aerospace, automotive, and defence industries. RTM is a promising process to obtain complex-shaped, high-quality product without using large equipment. In RTM, the preform is placed in the mold, and then the viscous resin is injected into the cavity and cured. The resin impregnation stage often results in the formation of a dry spot, a region where the resin does not impregnate into the preform. Usually, many trials are required to eliminate the dry spot. As the shape of the product becomes more complex, determining the process parameters by trial-and-error becomes too expensive.

Two approaches have been taken to prevent the formation of a dry spot during the RTM process. One is to determine the process parameters by numerical simulation. Numerical simulation is a powerful tool for determining the appropriate numbers and locations of the resin injection gates and vents, and the injection

*To whom correspondence should be addressed. E-mail: takashi_itou_3@ihi.co.jp

pressure in the case of the multiple injection [1–3]. The impregnation process is described by Darcy's law, and the calculation is based on the control volumes [4, 5] or nonconforming finite elements [6, 7]. Permeability, a coefficient in Darcy's law, is an important parameter, but it is difficult to obtain the actual value experimentally [8, 9]. The inaccuracy of permeability sometimes leads to multiple certifying experiments.

The other approach is *in-situ* control of the parameters, using a sensor to monitor the resin-flow front. Methods used to monitor the position of the resin-flow front have been based on electrical resistance [1, 10–14], electrical capacitance [15], optical reflection [2], and dielectrometry [16–18]. Additionally, *in-situ* process control has been suggested by several authors [1, 2]. However, these sensors only provide point data, and thus a large number of sensors seem to have been located in the mold in order to fabricate a large complex-shaped product.

In this study, we propose the smart manufacturing technique of RTM integrated with numerical simulation, monitoring, and process control. The preliminary process parameters were determined using numerical simulation; the resin-impregnation process was controlled using dielectric sensors, which continuously monitored the progress of the resin-flow front [19–21]. This paper reports the procedure of the smart manufacturing process and demonstrates its performance by fabricating an access door panel model of a fuselage structure, which was fabricated as a damage detection and damage suppression demonstrator under the 'Smart Materials and Structure Systems' project [22].

2. FUNDAMENTALS OF SMART MANUFACTURING

2.1. Numerical simulation

The resin flow through the preform is assumed to be equivalent to the flow through a porous media. Darcy's law is used as the governing equation describing these conditions and is expressed as:

$$v_i = -\frac{k_{ij}}{\mu}\frac{\partial P}{\partial x_j}, \tag{1}$$

where v_i is the fluid velocity; k_{ij} is permeability, which depends on a porous media; μ is fluid viscosity; and P is pressure. In this study, the permeability was assumed to be isotropic since the crimp states of the warp and weft in the fabric were identical. The permeability used for the simulation was determined by a one-dimensional flow test, where the flow-front position and the filling time were measured using a transparent mold. PAM-RTM developed by the ESI group was used to predict the resin-flow behavior. The calculation results were confirmed to accurately describe the actual two-dimensional flow [3].

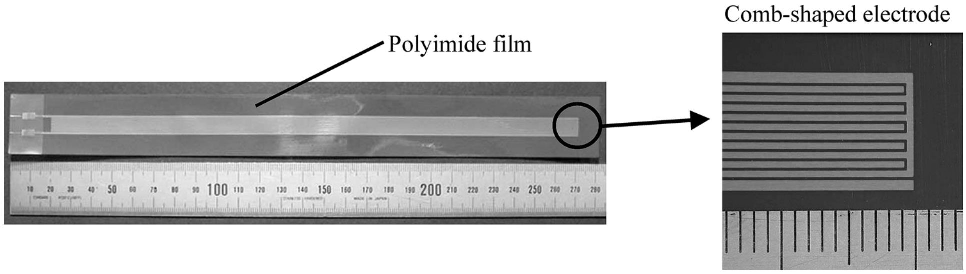

Figure 1. Dielectric film sensor installed the comb-shaped electrode.

2.2. Monitoring of the resin-flow front

A dielectric film sensor developed by Motogi *et al.* [19–21] was applied to monitor the position of the resin-flow front. The sensor's comb-shaped electrode was placed between thin polyimide films, as shown in Fig. 1. When an alternating voltage was applied to one of the electrodes, the amplitude of the voltage induced in the other electrode decreased and shifted phase angle. This behavior depended on the configuration of the electrodes and the dielectric properties of the medium between the electrodes. Dielectric constant, ε^*, is expressed as follows:

$$\varepsilon^* = \varepsilon' + i\varepsilon'', \tag{2}$$

where the real part (ε') is permittivity and the imaginary part (ε'') is the loss factor. Figure 2 presents the experimental results, where the dielectric film sensor was immersed into the resin bath. The permittivity, measured by the dielectrometer (Eumetric 100A, Holometrix-Micromet Instruments), was proportional to the length of the immersed part of the sensor. The position of the resin-flow front in the mold was continuously acquired by using this sensor.

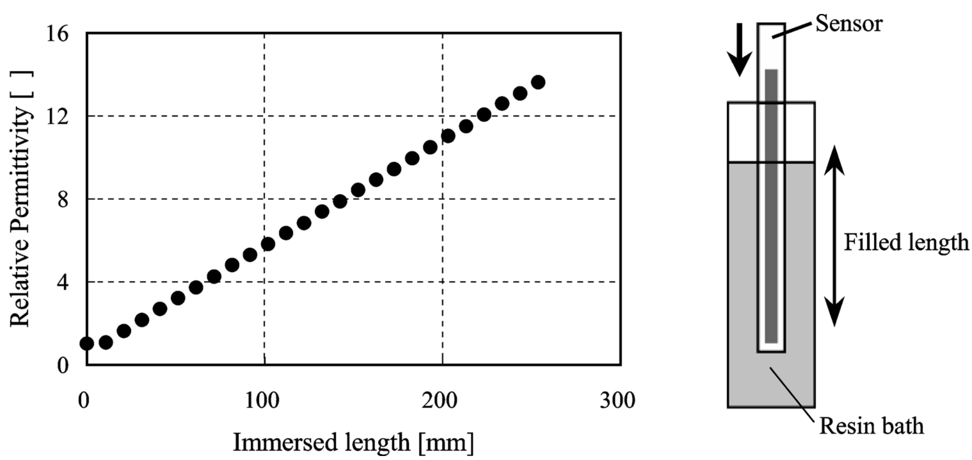

Figure 2. Detection of the resin flow front using the dielectric sensor.

2.3. In-situ *process control*

Figure 3 schematically illustrates the monitoring and control system. Four injection lines and four sensors were installed in the system. The resin was stored in the four pressure pots, which were connected to the compressed air source. The four dielectric sensors were placed along the resin-flow direction. The personal computer received the data from the dielectrometer and controlled the injection pressure at the each gate, comparing it with the ideal data predicted through simulation.

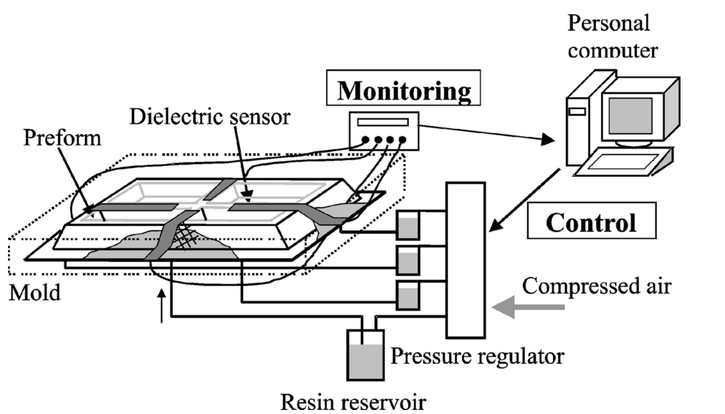

Figure 3. Schematic of the monitoring and control system.

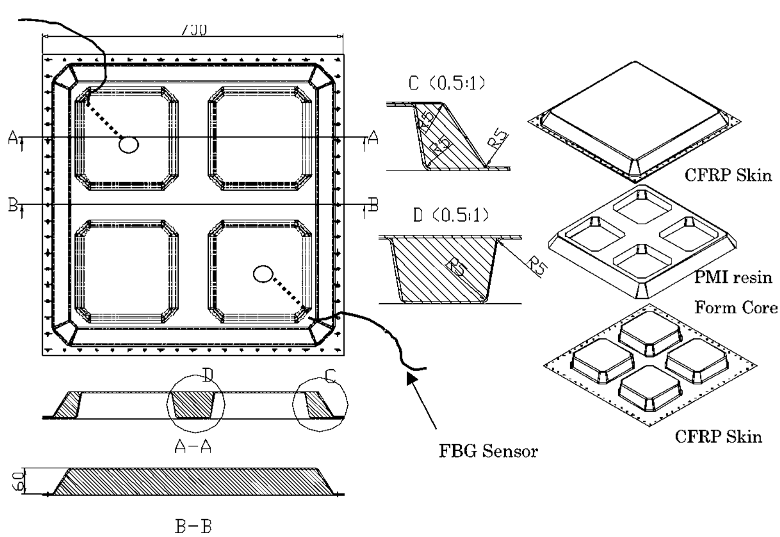

Figure 4. Scaled model of the access door panel for the airliner fuselage structure.

3. ACCESS DOOR PANEL MODEL

3.1. Fabrication and evaluation

Figure 4 depicts the schematic of the access door panel model. The panel was 700 mm wide and 60 mm thick; its girder was composed of CFRP skin and a polymethacrylimide foam core (ROHACELL WF-71). Four plies of carbon fabric (TORAY CO6341, 8 harness satin fabric) were used as the preforms for the upper and lower skins. The panel was a part of the fuselage structure model, fabricated as the damage detection and damage suppression demonstrator under the 'Smart Materials and Structure Systems' project [22]. Fiber Bragg grating (FBG) sensors (Advanced Optics Solutions GmbH, 1550 nm peak-wavelength, 125 μm diameter)

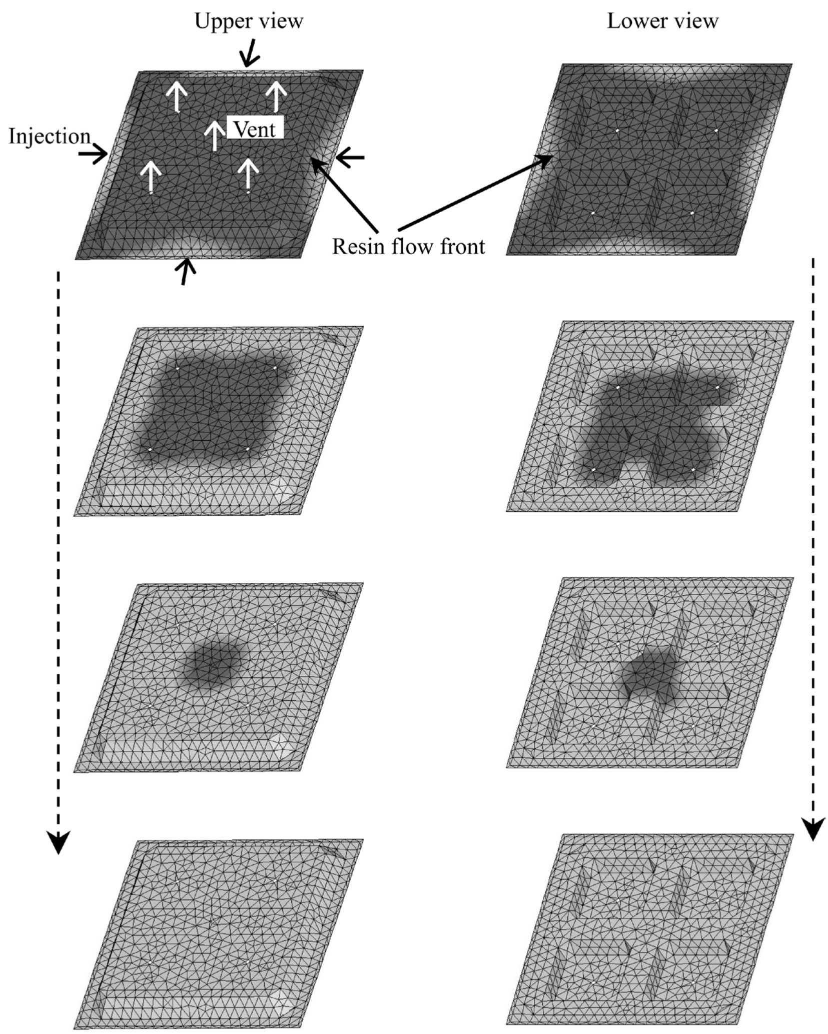

Figure 5. Result of the resin flow simulation.

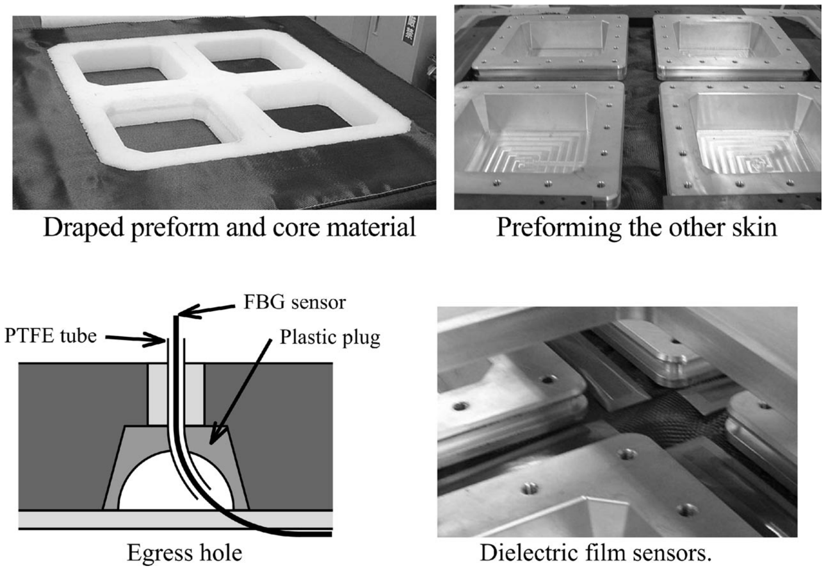

Figure 6. Preforming and setting up the sensors.

were embedded in the maximum strain region for internal pressure testing to verify the demonstrator. The FBG sensor monitored the internal strain by using the wavelength shift of the reflected light at the fiber grating.

The number and location of the gates and vents were determined after a few calculations. Figure 5 shows the result of the resin-flow simulation of the panel under optimized conditions. There were no dry spots in the panel. Figure 6 illustrates the preforming procedure. To maintain the continuity of the fiber tow, the preforms were draped into each shape without being cut. The FBG sensors were knitted in the preform of the upper skin, and the foam core was placed between the upper and lower skins. Handling the FBG sensor at ingress/egress points is problematic, since the optical fiber is easily damaged there. In this study, the FBG sensors were drawn from the surface of the preform, and the egress hole of the mold was sealed with a plastic plug [23]. The four dielectric film sensors were placed on the preform along the girders. After the preforming, the resin was injected into the mold, and the resin was cured after the preforms were saturated with the resin. The resin impregnation took 40 minutes.

Figure 7 depicts the fabricated access door panel model. Ultrasonic non-destructive evaluation was conducted to verify the absence of dry spots in the panel. Figure 8 illustrates one of the ultrasonic c-scan results. These results indicated no dry spot exceeding 0.7 mm (the diameter of the focused ultrasonic beam) in the panel.

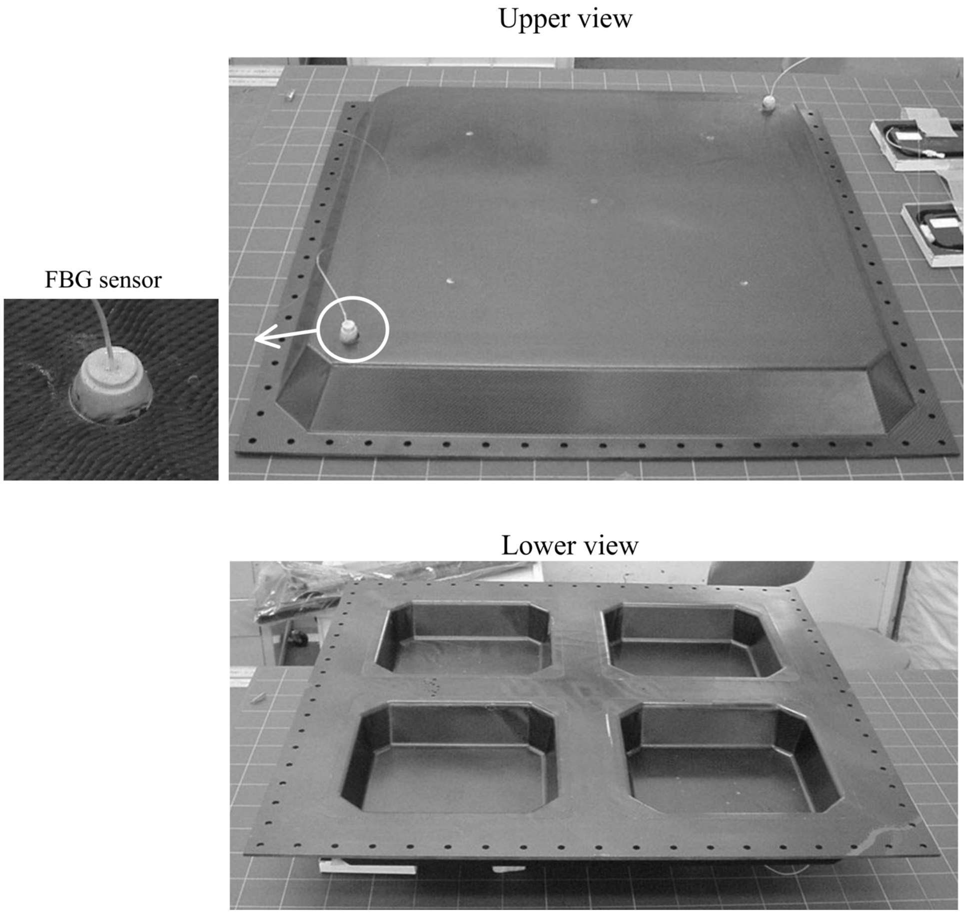

Figure 7. Access door panel model embedded with the FBG sensors.

3.2. Internal pressure test

The panel was attached to the bulkhead of the fuselage structure model and subjected to internal pressure. Figure 9 shows the experiment set-up of the internal pressure test. The maximum internal pressure was 75 kPa. The strain gage was glued to the surface of the panel for comparison with the internal strain monitored by the FBG sensor. Figure 10 presents the results of the applied internal pressure and the strain monitored by the FBG sensor and the strain gage. The strain of the FBG sensor was slightly lower than that of the strain gage at the surface because the FBG sensor was embedded in the panel. The FBG sensor was embedded at a distance of 2.0 mm from the neutral surface; the strain gage was embedded 2.3 mm from it. The distance ratio of FBG sensor and strain gage was 0.86, which was almost equal to the strain ratio (0.89). We thus confirmed that the embedded FBG sensor successfully monitored the internal strain of the panel.

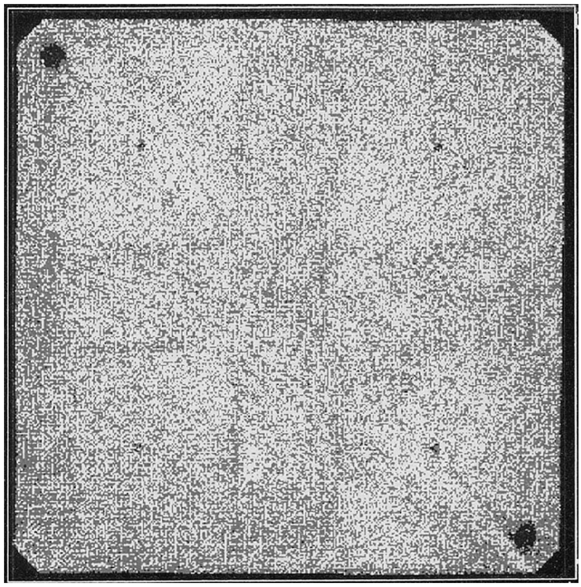

Figure 8. Ultrasonic c-scan result (top view).

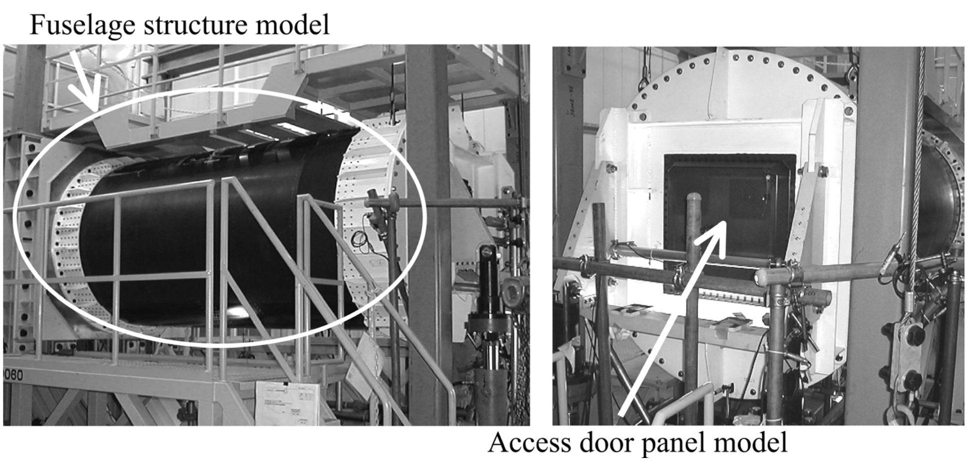

Figure 9. Damage detection and damage suppression demonstrator.

4. CONCLUSION

In this paper, we proposed smart manufacturing consisting of numerical simulation, process monitoring, and process control. The resin impregnation behavior was predicted using numerical simulation, and the appropriate process parameters were determined. A dielectric film sensor was used to continuously monitor the resin-flow front. The injection pressure was controlled using dielectric film sensors through fabricating an access door panel model of the fuselage structure model, embedded with the FBG sensor. The ultrasonic c-scan results indicated no dry spots

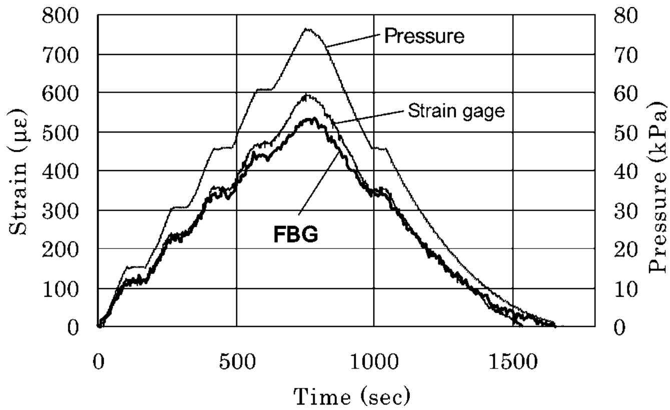

Figure 10. Monitored strains and internal pressure during the internal pressure test.

in the panel; the FBG sensor successfully monitored the internal strain during the internal pressure test.

Acknowledgement

We gratefully acknowledge the support of NEDO (New Energy and Industrial Development Organization) and RIMCOF (R&D Institute of Metals and Composites for Future Industries), Japan.

REFERENCES

1. S. Bickerton, H. C. Stadtfeld, K. V. Steiner and S. G. Advani, Design and application of actively controlled injection schemes for resin-transfer molding, *Compos. Sci. Technol.* **61**, 1625–1637 (2001).
2. M. K. Kang, J. J. Jung and W. I. Lee, Analysis of resin transfer moulding process with controlled multiple gates resin injection, *Composites* **31A**, 407–422 (2000).
3. M. Y. Lin, M. J. Murphy and H. T. Hahn, Resin transfer molding process optimization, *Composites* **31A**, 361–371 (2000).
4. M. K. Kang and W. I. Lee, A flow-front refinement technique for the numerical simulation of the resin transfer molding process, *Compos. Sci. Technol.* **59**, 1663–1674 (1999).
5. M. Y. Lin, M. K. Kang and H. T. Hahn, A finite element analysis of convection problems in RTM using internal nodes, *Composites* **31A**, 373–383 (2000).
6. F. Trochu, P. Ferland and R. Gauvin, Functional requirements of a simulation software for liquid molding process, *Sci. Engng Compos. Mater.* **16**, 209–218 (1997).
7. M. L. Diallo, R. Gauvin and F. Trochu, Experimental analysis and simulation of flow through multi-layer fiber reinforcements in liquid composite molding, *Polym. Compos.* **19**, 246–256 (1998).
8. R. Gauvin, F. Trochu, Y. Lemenn and L. Diallo, Permeability measurement and flow simulation through fiber reinforcement, *Polym. Compos.* **17**, 34–42 (1996).
9. R. Gauvin and F. Trochu, Key issues in numerical simulation for liquid composite molding process, *Polym. Compos.* **19**, 233–240 (1998).

10. M. Devillard, K.-T. Hsiao, A. Gokce and S. G. Advani, On-line characterization of bulk permeability and race-tracking during the filling stage in resin transfer molding process, *J. Compos. Mater.* **37**, 1525–1541 (2003).
11. S. M. Walsh, In-situ sensor method and device, US Patent No. 5,210,499 (1993).
12. S. M. Walsh and C. E. Freese, Resin flow front reconstruction with applications to resin transfer molding, in: *41st Intern. SAMPE Symp.*, pp. 1486–1495 (1996).
13. S. D. Schwab, R. L. Levy and G. G. Glover, Sensor system for monitoring impregnation and cure during resin transfer molding, *Polym. Compos.* **17**, 312–317 (1996).
14. D. D. Shepard, A new instrument for monitoring the resin flow front and cure in RTM and other resin infusion process, in: *International Composites Expo '98*, 1-5/session 2-A (1998).
15. D. E. Kranbuehl, P. Kingsley, S. Hart, G. Hasko, B. Dexter and A. C. Loos, In situ monitoring and intelligent control of the reisn transfer molding process, *Polym. Compos.* **15**, 299–305 (1994).
16. K. N. Kendal, Flow and cure phenomena in liquid composite molding, *Polym. Compos.* **15**, 334–348 (1994).
17. A. Mcllhagger, D. Brown and B. Hill, The development of a dielectric system for the on-line cure monitoring of the resin transfer moulding process, *Composites* **31A**, 1373–1381 (2000).
18. D. Kranbuehl, P. Kingsley, S. Hart, A. Loos, G. Hasko and B. Dexter, Sensor-model prediction, monitoring and in-situ control of liquid RTM advanced fiber architecture composite processing, in: *37th Intern. SAMPE Symp.*, pp. 907–913 (1992).
19. S. Motogi, T. Itoh, T. Fukuda, K. Yamagishi, S. Kitade and H. Morita, Development of multi-functional sensor in resin transfer molding, in: *12th Intern. Conf. on Composite Materials*, Paris, France (1999).
20. S. Motogi, T. Itoh and T. Fukuda, Multi-functional sensor properties and 2-Dim flow detection for RTM, in: *6th Japan Intern. SAMPE Symp.* (1999).
21. S. Motogi, K. Yamagishi and T. Fukuda, Novel sensor development for resin front detection in RTM, in: *2nd Asian–Australasian Conference on Composite Materials*, Tokyo, Japan (2000).
22. N. Tajima, T. Sakurai, M. Sasajima, N. Takeda and T. Kishi, Overview of demonstrator program of Japanese smart materials and structures system project, in: *SPIE Smart Structures and Materials 2003*, Vol. 5054, pp. 165–174 (2003).
23. T. Kosaka, K. Osaka and T. Fukuda, Cure and health monitoring of RTM molded FRP by using optical fiber strain sensors, in: *5th Intern. Conf. on Durability Analysis of Composite Systems*, Kyeong Ju, Korea, pp. 138–142 (2001).